J. Am. Chem. Soc. 1990, 112, 2915-2921

# Conformation and Stereodynamics of a Highly Hindered Ethane, 1,2-Bis(2,4,6-tri-*tert*-butylphenyl)ethane, and of the Corresponding Ethyl Radical[†]

**Mauro A. Cremonini,[1a] Lodovico Lunazzi,*[,1b] Giuseppe Placucci,*[,1b] Renji Okazaki,[1c] and Gaku Yamamoto[1c]**

*Contribution from the Dipartimento di Chimica Organica "A. Mangini", University of Bologna, Risorgimento, 4 Bologna 40136, Italy, and Department of Chemistry, Faculty of Science, The University of Tokyo, Bunkyo-ku, Tokyo 113, Japan.* *Received August 1, 1989*

**Abstract:** The variable-temperature dynamic NMR spectra of the title compound (**1**, $ArCH_2CH_2Ar$, where Ar = 2,4,6-tri-*tert*-butylphenyl) allowed the free energy of activation ($\Delta G^{*}$ = 12.9 kcal mol$^{-1}$) to be determined for the internal molecular motions. Molecular mechanics calculations indicate that **1** adopts the same eclipsed conformation as found in an X-ray diffraction study. These calculations also show that the internal motion is due to $CH_2$–$CH_2$ rotation highly correlated with Ar–$CH_2$ rotation. The computed pathway for this process predicts that $CH_2$–$CH_2$ rotation is accompanied by rotation about one of the Ar–$CH_2$ bonds. This conclusion has been confirmed by the experimental observation that the rate constant determined, at a given temperature, for the $CH_2$–$CH_2$ rotation is *twice* as large as that determined for the Ar–$CH_2$ rotation. In the analogous disulfide **3** ($ArCH_2SSCH_2Ar$) no such correlated motion exists and the barrier ($\Delta G^{*}$ = 8.15 kcal mol$^{-1}$) is that of an isolated S–S rotation. The rate constants determined by monitoring the $CH_2$ signal of **3** are in fact equal to those obtained by monitoring the *tert*-butyl signal at the same temperature, as opposed to the case of **1**. In the corresponding ethyl radical, line-width alternation of the ESR spectra yields the activation parameters for the $\dot{C}H$–$CH_2$ rotation ($\Delta G^{*}$ = 6.3 kcal mol$^{-1}$, $\Delta H^{*}$ = 6.3 kcal mol$^{-1}$, $\Delta S^{*}$ = −0.2 eu). Analysis of the hyperfine splittings suggests that the conformation of the radical is staggered, with the Ar–$CH_2$ bond making an angle of 56° with the $p_z$ orbital of the $sp^2$ carbon bearing the unpaired electron. There is also an indication that, despite the crowded situation, there is still conjugation between the Ar group and the radical center.

Restricted rotation about the $sp^3$–$sp^3$ bond in hydrocarbons has been detected by NMR only when tertiary or quaternary carbons are involved. Examples of this type are, for instance, $Me_2CH$–$CHMe_2$ ($\Delta G^{*}$ = 4.3 kcal mol$^{-1}$),[2] where both carbons are tertiary atoms, $^tBu_2MeC$–$CHMe_2$ ($\Delta G^{*}$ = 8.9 kcal mol$^{-1}$),[3] where one carbon is tertiary and the other quaternary, and $EtMe_2C$–$CMe_2Et$ ($\Delta G^{*}$ = 10.6 kcal mol$^{-1}$),[4] where both carbons are quaternary. Internal rotation in 1,2-dialkyl-substituted ethanes ($RCH_2$–$CH_2R$) in solution has never been observed by NMR, most likely because the steric hindrance is too small when both carbons are secondary. Here we report the first example of a rotational barrier measured by NMR in solution in this class of compounds.

## Results and Discussion

**NMR and Molecular Mechanics Investigations.** 1,2-Bis-(2,4,6-tri-*tert*-butylphenyl)ethane (**1**) displays proton NMR spectra (200 MHz) where the singlet signals corresponding, respectively, to the four methylene hydrogens, to the four meta hydrogens, and to the 36 hydrogens of the ortho *tert*-butyl groups split into a pair of equally intense groups of signals below 0 °C (Table I). In particular, the methylene protons yield four lines at −50 °C (Figure 1), typical of an AA′BB′ spectrum closely approaching an AB pattern, where only the geminal coupling constant ($J$ = 11.5 Hz) is observed. The protons in the meta positions yield, on the other hand, a genuine AB spectrum ($J$ = 1.9 Hz); the line widths of these signals are in fact much sharper than those of the methylene hydrogens since the signals of the latter group also contain the unresolved transitions expected for an AA′BB′ spectrum.

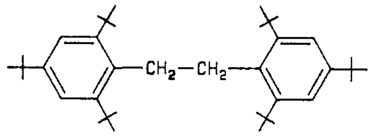

**1**

The reversible, temperature-dependent exchange process observed in the NMR spectra can be, in principle, explained by taking into account two possible motions: (i) restricted rotation about the Ar–$CH_2$ bond and (ii) restricted rotation about the $CH_2$–$CH_2$ bond. Let us assume, for the time being, that the two motions are independent of each other.

(i) Restricted Ar–$CH_2$ rotation has been reported in a variety of derivatives.[5–9] In all the cases reported so far, however, the molecules had a lower symmetry than **1** (the two ortho substituents were never equal to each other, unlike the present case). In principle, four conformers (A–D in Chart I)[10] might be considered

**Chart I**

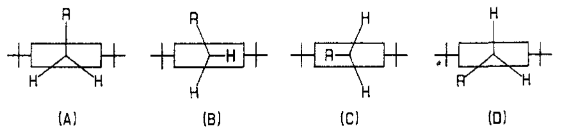

R = $ArCH_2$ ; Ar = 2,4,6-tri-tert-butylphenyl

**Chart II**

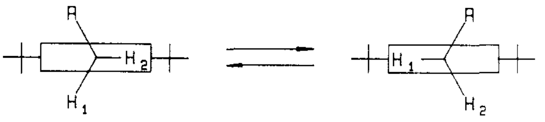

R = $ArCH_2$: Ar = 2,4,6-tri-tert-butylphenyl

---

[†] Dedicated to the memory of Prof. G. Maccagnani (1935–1989).

[1] (a) Taken, in part, from: Cremonini, M. A. Doctoral Thesis, Industrial Chemistry, University of Bologna. (b) University of Bologna. (c) University of Tokyo.

[2] Lunazzi, L.; Macciantelli, D.; Bernardi, F.; Ingold, K. U. *J. Am. Chem. Soc.* **1977**, *99*, 4573.

[3] Anderson, J. E.; Bettels, B. R.; Hoffmann, H. M. R.; Pauluth, D.; Hellmann, S.; Beckhaus, H.-D.; Ruchardt, C. *Tetrahedron* **1988**, *44*, 3701.

[4] Beckhaus, H.-D.; Ruchardt, C.; Anderson, J. E. *Tetrahedron* **1982**, *38*, 2299.

[5] Cupas, C. A.; Bollinger, J. M.; Haslanger, M. *J. Am. Chem. Soc.* **1968**, *90*, 5502.

[6] Nilsson, B.; Martinson, P.; Olsson, K.; Carter, R. E. *J. Am. Chem. Soc.* **1974**, *96*, 3190.

[7] Elzinga, J.; Hogeveen, H. *J. Org. Chem.* **1981**, *46*, 1353.

[8] Anderson, J. E.; Barkel, D. J. D. *J. Chem. Soc., Perkin Trans. 2* **1984**, 1503.

[9] Anderson, J. E.; Barkel, D. J. D.; Jorgensen, F. S. *J. Chem. Soc., Perkin Trans. 2* **1988**, 199.

0002-7863/90/1512-2915$02.50/0

**Table I.** Proton Chemical Shifts (ppm at 200 MHz) of Compounds **1**–**3** Measured at Low Temperatures

| | | proton shifts, ppm | | | | | | |
|---|---|---|---|---|---|---|---|---|
| compd | temp, °C | o-Bu$^t$ | o′-Bu$^t$ | p-Bu$^t$ | CH | CH | m-H | m′-H |
| **1** (in $CD_2Cl_2$)[a] | −50 | 0.86 | 1.54 | 1.25 | 2.88 | 3.74 | 7.03 | 7.37 |
| **2** (in $CD_2Cl_2$) | −110 | 1.55 | 1.55 | 1.25 | 4.50 | 4.50 | 7.40 | 7.40 |
| **2** (in $CHFCl_2/CCl_2F_2$) | −130 | 1.55 | 1.55 | 1.25 | 4.45 | 4.45 | | |
| **3** (in $CD_2Cl_2/CHF_2Cl$)[b] | −120 | 1.64 | 1.76 | 1.47 | 4.75 | 5.22 | | |

[a] The $\Delta G^{\ddagger}$ for the $CH_2$–$CH_2$ rotation and for the Ar–$CH_2$ rotation are given in Table II. [b] The $\Delta G^{\ddagger}$ for the S–S rotation is 8.15 ± 0.15 kcal mol$^{-1}$, at −110 °C.

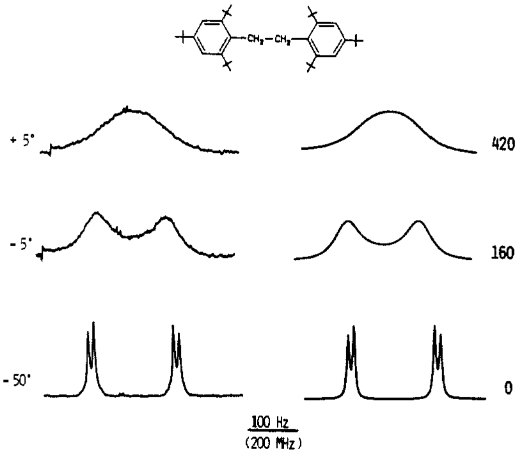

**Figure 1.** Experimental (left) and computed (right) proton NMR signals (200 MHz) of the methylene hydrogens of hydrocarbon **1** in $CD_2Cl_2$ at various temperatures. The rate constants ($k$, s$^{-1}$) used for the simulations are also reported.

as representing the possible rotational ground states of **1**.

Conformers A and C, owing to their symmetry, cannot account for the whole set of different shifts observed at low temperatures. The conformation adopted by **1** in the crystal (X-ray diffraction)[11a] is actually conformation B, with the two C–H bonds of the methylene group displaying dihedral angles of −63.0 and 5.8°, respectively, with the plane of the phenyl ring.[11b] If the same conformation B is maintained also in solution, a 60° clockwise rotation about the Ar–$CH_2$ bond might account for the exchange of all the nonequivalent NMR signals, provided the rotation about the $CH_2$–$CH_2$ bond is much faster. If this is the case, the latter rotation would not affect the spectral line widths in the temperature range examined. The motion is represented in Chart II, where H-1 takes the place of H-2, and at the same time, the *tert*-butyl groups and the meta hydrogens exchange their chemical shifts with the *same* rate constant of the methylene hydrogens.

(ii) Conversely, a rotation about the $CH_2$–$CH_2$ bond might also explain the experimental findings, provided two additional conditions are also fulfilled. The first one requires that the conformer has the same type of symmetry as that of a gauche conformer (Chart III).

The symmetry of the anti conformer would in fact render the four methylene hydrogens equivalent, either when the $CH_2$–$CH_2$ rotation is fast or when it is slow. This is not the case for the gauche conformer where two types of hydrogens (inner and outer) might be observed in the slow-exchange region. The second condition requires that other possible motions that might cause the diastereotopicity of the methylene protons are ineffective and solely the restricted $CH_2$–$CH_2$ rotation is responsible for the observed nonequivalence. In other words, the Ar–$CH_2$ arrangement must be either of type A or, if it is of type B, the equilibration shown in Chart I has to be faster than the $CH_2$–$CH_2$ rotation. Furthermore, it is also implied that the 180° rotation about the Ar–$CH_2$ bond (that would make the meta hydrogens and the ortho *tert*-butyl groups homotopic even in a gauche conformer) has a higher energy than the $CH_2$–$CH_2$ rotation. Under these circumstances the meta hydrogens and the ortho *tert*-butyl groups can be diastereotopic in a gauche conformer, when the $CH_2$–$CH_2$ rotation is slow, and would exhange with rate constants *equal* to those of the methylene hydrogens at the same temperature.

**Chart III**

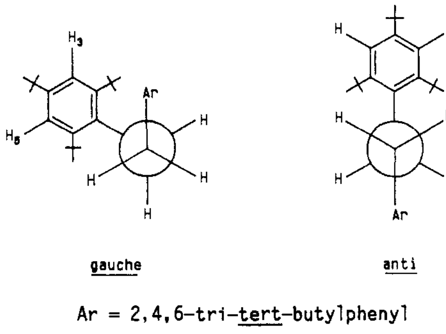

**Table II.** Rate Constants of Exchange (in s$^{-1}$) at Various Temperatures and NMR Parameters for the Three Groups of Proton Signals of **1** in $CD_2Cl_2$ at 200 MHz

| | −10 °C | −5 °C | 0 °C | +5 °C | $\Delta\nu$[a] | $\Delta G^{\ddagger}$,[b] |
|---|---|---|---|---|---|---|
| $k(CH_2)$ | 100 | 160 | 260 | 420 | 173 | 12.9 |
| $k$(m-H) | 50 | 95 | 140 | 220 | 69 | 13.2 |
| $k$(t-Bu) | 54 | 95 | 135 | 210 | 137 | 13.2 |

[a] Internal chemical shift difference in hertz, measured at −50 °C. [b] Averaged free energy of activation for the correlated internal motion in kilocalories per mole. The differences between the values measured at four temperatures do not exceed 0.1 kcal mol$^{-1}$.

The X-ray structure[11] indicates that the Ar–C–C–Ar dihedral angle of **1** is 119.9°: this corresponds to an eclipsed conformation that has, however, the same type of symmetry as a gauche conformation and might as well account for the nonequivalence of the low-temperature NMR signals. Also the condition of a fast 60° Ar–$CH_2$ rotation (Chart II) and of a slow 180° Ar–$CH_2$ rotation might be conceivably met in such a hindered Ar–$CH_2$ moiety.

Both hypotheses i and ii seem therefore acceptable, in principle, although they have opposite requirements in that, in i, the 60° Ar–$CH_2$ rotation of conformer B (Charts I and II) should have a *higher* energy than the $CH_2$–$CH_2$ rotation, whereas, in ii, the 60° Ar–$CH_2$ rotation of conformer B should have an energy *lower* than the $CH_2$–$CH_2$ rotation. Careful examination of the NMR traces does show, however, that the computer simulation of the methylene signals could be achieved *only* using rate constants *twice* as large as those required to simulate the shapes of signals due both to the meta hydrogens and to the ortho *tert*-butyl groups (Table II). Clearly neither of the two simple models previously discussed, where only a single motion had been considered responsible for the low-temperature NMR features, can explain the experimental findings.

In order to have a better understanding of the complex stereodynamics of this hindered hydrocarbon and in order to clarify the NMR observations, molecular mechanics calculations were applied to **1** using the MM2 program.[12] To simplify the calcu-

---

(10) Ōki, M. *Applications of Dynamic NMR Spectroscopy to Organic Chemistry*; VCH Publishers: Deerfield Beach, FL, 1985; p 194.

(11) (a) Winter, W.; Butters, T.; Rieker, A.; Butsugan, Y. *Z. Naturforsch.* **1982**, *37B*, 855. (b) Winter, W., private communication based upon unpublished data of ref 11a.

**Table III.** Bond Lengths, Bond Angles, and Dihedral Angles[a] of Hydrocarbon **1** Obtained from MM2 Computation (calcd) and X-ray Diffraction[11] (obsd)

| | bond length, Å | | | bond angle, deg | | | dihedral angle, deg | |
|---|---|---|---|---|---|---|---|---|
| | calcd | obsd | | calcd | obsd | | calcd | obsd[b] |
| 7–22 | 1.553 | 1.567 | 1–7–22 | 116.4 | 112.6 | 1–7–22–16 | 101.1 | 119.9 |
| 1–7 | 1.524 | 1.518 | 7–1–2 | 120.2 | 119.3 | 2–1–7–22 | −108.2 | −115.0 |
| 1–2 | 1.429 | 1.426 | 7–1–26 | 119.2 | 121.5 | 6–1–7–22 | 70.9 | 57.8 |
| 2–3 | 1.403 | 1.390 | 1–2–9 | 126.8 | 123.9 | 7–1–2–9 | −10.2 | −18.0 |
| 3–4 | 1.385 | 1.392 | 1–6–13 | 129.9 | 127.8 | 7–1–6–13 | 8.4 | 18.6 |
| 4–5 | 1.385 | 1.379 | 2–9–8 | 113.8 | 112.1 | 1–2–9–8 | 65.2 | 76.2 |
| 5–6 | 1.404 | 1.399 | 2–9–10 | 109.7 | 111.4 | 1–2–9–10 | −61.9 | −49.5 |
| 1–6 | 1.428 | 1.417 | 2–9–11 | 114.3 | 111.3 | 1–2–9–11 | −177.2 | −165.8 |
| 2–9 | 1.558 | 1.557 | 6–13–12 | 109.3 | 110.4 | 1–6–13–12 | −109.9 | −105.4 |
| 9–8 | 1.543 | 1.540 | 6–13–14 | 109.0 | 109.0 | 1–6–13–14 | 131.8 | 136.7 |
| 9–10 | 1.549 | 1.543 | 6–13–15 | 120.2 | 116.1 | 1–6–13–15 | 14.8 | 19.4 |
| 9–11 | 1.561 | 1.541 | | | | 2–1–7–35 | 15.6 | 5.8 |
| 6–13 | 1.561 | 1.559 | | | | 6–1–7–34 | −56.7 | −63.0 |
| 13–12 | 1.546 | 1.540 | | | | | | |
| 13–14 | 1.560 | 1.550 | | | | | | |
| 13–15 | 1.546 | 1.532 | | | | | | |

[a] The numberings are shown in Figure 2. [b] Obtained from the positional parameters given in ref 11a.

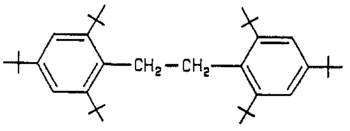

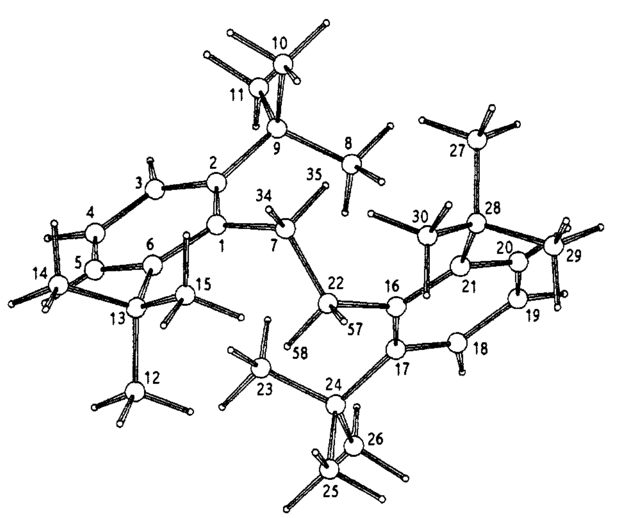

**Figure 2.** Structure of hydrocarbon **1** as obtained by the MM2 calculations. Some relevant structural parameters are reported in Table III.

lations the *tert*-butyl groups in the para positions were omitted. The ground-state conformation obtained is shown in Figure 2 and the relevant geometrical data are reported in Table III. The computed conformation is astonishingly close to that obtained by the X-ray investigation; the differences between the computed and the solid-state dihedral angles never exceed 20° (Table III) and are most likely due to the perturbations by the crystal packing forces in the solid state. In particular, the dihedral angle Ar–C–C–Ar (i.e., 1–7–22–16 of Figure 2) indicates that the molecule prefers indeed to stay in an almost eclipsed conformation, as shown by the Newman projection in Chart IV.

Such a situation is not unprecedented and has been found in highly crowded tetra-substituted ethanes,[2,13] but the present case seems to be the first example in a 1,2-disubstituted ethane. Also, the dihedral angle formed by one of the two methylene bonds with the phenyl ring (i.e., 6–1–7–34) confirms that the preferred conformation is of type B (computed −56.7°, X-ray −63°). In other words, the arrangement adopted in the crystal seems to be essentially maintained also in the isolated molecule, hence also in solution.

**Chart IV**

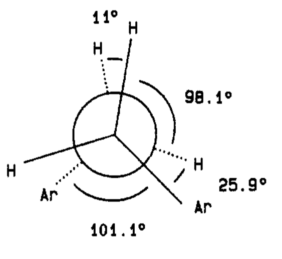

**Chart V**

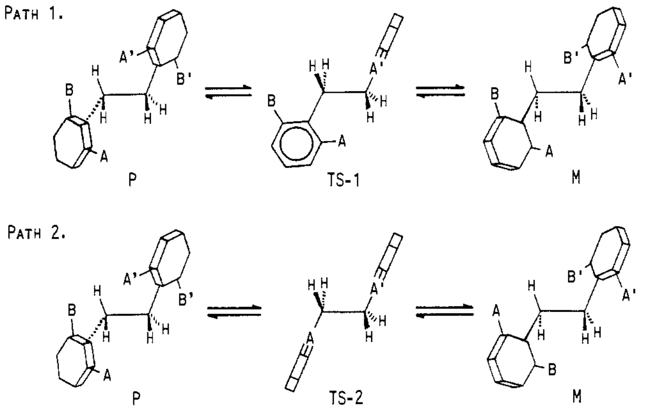

The dynamic process observed by variable-temperature NMR corresponds to the interconversion between the ground-state conformation of **1** (*P* in Chart V) and its antipode (*M* in Chart V). The rotational itinerary was studied with the MM2 method by driving the central $CH_2$–$CH_2$ bond and allowing, at the same time, the molecule to minimize its energy as for the other degrees of freedom.

The calculations show that the internal motions of the molecule are highly correlated. The most favorable pathway was found to be the one occurring through a rotational transition state, where the two aryl moieties are in an anti arrangement with respect to the central $CH_2$–$CH_2$ bond, as shown in path 1 of Chart V. This transition state (indicated as TS-1) corresponds to a saddle point in the energy surface and it lies 13.19 kcal mol$^{-1}$ above the ground state (either *P* or *M*).[14] It should be noticed that in the transition

---

(12) Allinger, N. L.; Yuh, Y. H. *QCPE No. 395.*

(13) Hounshell, W. D.; Dougherty, D. A.; Mislow, K. *J. Am. Chem. Soc.* **1978**, *100*, 3149. Ōsawa, E.; Shirahama, H.; Matsumoto, T. *J. Am. Chem. Soc.* **1979**, *101*, 4824.

(14) A plane of symmetry was assumd for transition states. Although such an element of symmetry is not a prerequisite, it is obvious that the chirality of the molecule should invert somewhere during the transformation of *P* into *M*.

**Table IV.** Hyperfine Splitting Constants ($a_H$ in Gauss) and $g$ Factors for the Radical $Ar\dot{C}HCH_2Ar$ (**4**, Ar = 2,4,6-tri-*tert*-butylphenyl) and for Its Labeled Derivative **4d**[a]

| radical | temp, °C | H-3[b] | H-5[b] | $H_\alpha$ | $H_\beta$ | $H_\beta'$ | $g$ factor | $\Delta G^{\ddagger c}$ |
|---|---|---|---|---|---|---|---|---|
| 4 | −100 | 1.75 | 2.6 | 14.25 | 7.4 | 25.9 | 2.0030 | 6.3 ± 0.15[d] |
| **4d** | −100 | | | 14.3 | 7.4 | 25.95 | 2.0030 | 6.3 ± 0.15[d] |

[a] See text. [b] Splittings of the meta hydrogens of the Ar group bonded to CH. Those of the Ar group bonded to $CH_2$ are zero. [c] Averaged free energy of activation (kcal mol$^{-1}$) corresponding to the $\dot{C}H-CH_2$ rotational process. [d] $\Delta H^{\ddagger} = 6.3 \pm 0.3$ kcal mol$^{-1}$, $\Delta S^{\ddagger} = -0.2 \pm 1.0$ eu from 12 $\Delta G^{\ddagger}$ values between −60 and +61 °C.

state TS-1, one of the two aryl groups is coplanar with the central bond (i.e., the dihedral angle 6–1–7–22 is 0°) whereas the other is perpendicular (i.e., 17–16–22–7 is 90°).

Another possible pathway (i.e., path 2 of Chart V) can also occur through an anti transition state (TS-2). In this case both the aryl groups are perpendicular with respect to the central bond, hence parallel to each other.[14] However, the calculations indicate that such an arrangement has an energy 26.96 kcal mol$^{-1}$ higher than that of the ground state.

Finally, a third possible rotational pathway is that having a transition state with the two aryl groups in a syn rather than in an anti arrangement. The geometry of such a transition state could not be, however, attained within the framework of the MM2 program. The corresponding barrier was estimated to be at least 31.4 kcal mol$^{-1}$ and the pathway is thus even less likely than path 2.

In path 1, which is the one actually followed by the molecule, the two *tert*-butyl groups in one of the two aryl moieties (A′ and B′ in Chart V) exchange their magnetic environments whereas those in the other aryl moiety (A and B in Chart V) do not. Of course the probability that the pair of *tert*-butyl groups in one ring exchange, whereas those in the other do not, is the same as that for the opposite process (i.e., A,B exchanging and A′,B′ not exchanging). As a consequence, this process requires that the rate constant for the exchange of the *tert*-butyl groups (and for the meta hydrogens as well) is *one-half* of the rate constant for the exhange of the methylene hydrogens at the same temperature. This is exactly what was experimentally observed. Furthermore, the measured free energy of activation (Table II) matches remarkably well the computed energy difference (13.19 kcal mol$^{-1}$) between the transition state TS-1 and the ground state (*P* or *M* of path 1 of Chart V).

In order to give further evidence to the conclusion that the dynamic process in **1** entails a correlated motion involving both $Ar-CH_2$ and $CH_2-CH_2$ bonds, two analogous derivatives were subsequently investigated. They were chosen in such a way as to eliminate the possibilities of correlated motions, by introducing either a sulfur atom or a disulfide moiety between the two $Ar-CH_2$ moieties, i.e.:

$ArCH_2-S-CH_2Ar$ $ArCH_2-S-S-CH_2Ar$
**2** **3**

Ar = 2,4,6-tri-*tert*-butylphenyl

In sulfide **2** no dynamic effects were observed, by both $^1H$ and $^{13}C$ NMR (even at −130 °C). The $CH_2-S$ rotation is in fact a quite fast process that has never been slowed down on the NMR time scale. The lack of dynamic NMR features also indicates that either the $Ar-CH_2$ moiety of **2** is "locked" in the symmetric arrangement A of Chart I (R being now equal to $SCH_2Ar$) or the internal motion about the $Ar-CH_2$ bond (Chart II) is too fast to be detected. Molecular mechanics calculations suggest that in **2** the arrangement of the $Ar-CH_2$ moiety is very similar to that of **1**, i.e., it is of type B. The computed dihedral angle 6–1–7–34 is in fact −56° in **2**, comparable with −56.7° calculated for **1**. The calculations also indicate that the barrier for the 60° rotation (described in Chart II) which renders all sets of the hydrogens of the $ArCH_2$ moiety equivalent, is lower than 2 kcal mol$^{-1}$ in **2**. Since there is not here any correlated motion, all the hydrogen (and carbon) signals of **2** remain equivalent at any attainable temperature.

In the case of disulfide **3**, on the other hand, the low-temperature $^1H$ NMR spectra display diastereotopic methylene hydrogens and ortho *tert*-butyl groups[15] below −105 °C (Table I). The rate constants for the exchange of these signals are *equal* to each other at the same temperature (contrary to the case of **1**), thus indicating that a single motion is responsible for both the line-broadening effects. The $\Delta G^{\ddagger}$ value measured for this process is 8.15 kcal mol$^{-1}$, which is within the range of values reported[16] for disulfides of general formula $PhCH_2-SS-R$ (7–9.4 kcal mol$^{-1}$). The methylene hydrogens of **3** become in fact diastereotopic, as observed for those of the $PhCH_2-SS-R$ derivatives, when the S–S rotation is slow on the NMR time scale, because the C–S–S–C dihedral angle is ~90° and thus creates a center of asymmetry. The plane bisecting the $CH_2$ groups is not coincident, obviously, with any molecular plane of symmetry until the S–S rotation becomes fast enough as to create a dynamic molecular plane of symmetry (in **3** this occurs above −105 °C). The ortho *tert*-butyl groups can also be diastereotopic for exactly the same reason, provided the 180° rotation about the $Ar-CH_2$ bond has a barrier higher than that for the S–S rotation. In such circumstances the whole $Ar-CH_2$ system (and not only the methylene hydrogens, as in the unhindered $PhCH_2-SS-R$ derivatives) becomes a probe sensitive to the molecular asymmetry,[17] yielding, as a consequence, nonequivalent NMR signals. Molecular mechanics calculations indicate that in **3** the $ArCH_2$ moiety adopts an arrangement similar to those of **1** and **2** (the 6–1–7–34 dihedral angle being −49°), with a negligible barrier for the 60° rotation described in Chart II. On the other hand the barrier computed for a 180° rotation about the $Ar-CH_2$ bond (14.5 kcal mol$^{-1}$) is indeed higher than that computed for the S–S rotation (12 kcal mol$^{-1}$), thus accounting for the simultaneous nonequivalence of the $CH_2$ and *tert*-butyl NMR signals.

We may therefore conclude that when the correlation between the motions observed in **1** is lifted, as in the case of **2** and **3**, the restricted $Ar-CH_2$ rotation is not observed by NMR. As a consequence the low-temperature NMR spectra either monitor an isolated rotation (as S–S rotation in the case of **3**) or do not detect any internal motion (as in the case of **2**), when Ar is symmetric as in this investigation.

**ESR Study of the Ethyl Radical.** A quite interesting possibility would be that of studying the analogous rotational process also in radical **4**, where the $sp^3-sp^3$ bond between the two $CH_2$ groups has been transformed into an $sp^2-sp^3$ bond by elimination of one hydrogen atom from hydrocarbon **1**.

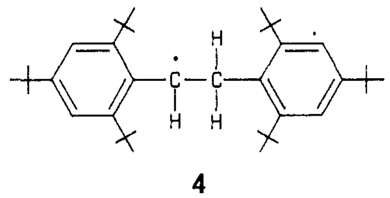

**4**

In **4** one would expect, in principle, that the rotations about the $CH_2-\dot{C}H$ and $Ar-\dot{C}H$ bonds be detectable through the selective line-broadening effects of the ESR spectral lines at various

---

(15) The meta hydrogens should also be diastereotopic. However, the corresponding chemical shift difference is probably smaller than the line width, which is quite broad (10 Hz) at the low temperatures required to detect this phenomenon. Furthermore this signal is, in part, obscured by that of $CHF_2Cl$ used as solvent to attain the required low temperature.

(16) Fraser, R. R.; Boussard, G.; Saunders, J. K.; Lambert, J. B.; Mixon, C. E. *J. Am. Chem. Soc.* **1971**, *93*, 3822.

(17) An analogous situation has been reported for the ortho methyl groups of twisted anilines containing an asymmetric center: Mannschreck, A.; Muensch, H. *Tetrahedron Lett.* **1968**, 3227.

**Chart VI**

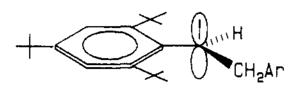

Ar = 2,4,6-tri-tert-butylphenyl

temperatures.[18-22] Radical **4** could not however be generated from hydrocarbon **1** in the usual way[23-27] (i.e., photolysis in the presence of di-*tert*-butyl peroxide). Most likely the steric congestion inhibits this reaction. A good steady-state ESR spectrum of **4** could, however, be obtained by photolysis in EtOH/EtOK of 2,4,6-tri-*tert*-butylthiobenzaldehyde[28] (ArCHS, where Ar = 2,4,6-tri-*tert*-butylphenyl). The mechanism explaining the generation of **4** from ArCHS will be discussed in detail elsewhere. The nature of radical **4** was assessed by product analysis (hydrocarbon **1**[11,27] was recovered from the photolysis of ArCHS in alkaline ethanol), by the consistency[18,27,29] of the ESR parameters (Table IV), and by the incorporation of deuterium when deuteriated species are employed.[30]

The low-temperature (−100 °C) ESR spectrum of **4** displays one hfs constant for the hydrogen bonded to the sp$^2$ carbon ($C_\alpha$) bearing the unpaired electron ($a_{H_\alpha}$ = 14.25 G), two different hfs constants (1.75 and 2.6 G) for the two meta hydrogens of the phenyl bonded to $C_\alpha$, and two different hfs constants (7.4 and 25.9 G) for the two methylenic hydrogens in position $\beta$ to the radical center. At temperatures higher than 80 °C the latter values tend to merge into an average $a_{H_\beta}$ splitting corresponding to two equivalent hydrogens, whereas the two meta hydrogens remain nonequivalent at any temperature. These features indicate that both $\mathrm{Ar{-}\dot{C}H}$ and $\mathrm{\dot{C}H{-}CH_2}$ rotations are restricted and also that the $\mathrm{Ar{-}\dot{C}H}$ barrier is too high to be determined. This agrees with the observations that the rates for the sp$^2$–sp$^2$ torsional process are too low on the time scale of the ESR technique, as shown by the different $H_2$,$H_6$ or $H_3$,$H_5$ splittings observed[28,31] at room temperature for many radicals of the type $\mathrm{\dot{C}{-}C_6H_5}$. Accordingly, the $\mathrm{Ar{-}\dot{C}H}$ fragment in **4** can be considered locked in a nearly coplanar conformation (Chart VI) in the whole temperature range.[27]

Whereas in the analogous radicals $\mathrm{Ar\dot{C}HS^-}$ or $\mathrm{Ar\dot{C}HO^-}$ (Ar = 2,4,6-tri-*tert*-butylphenyl) the two meta splittings are equivalent,[28] thus indicating an almost perpendicular arrangement between the sp$^2$ plane of the $\alpha$-carbon and the phenyl ring, the nonequivalence of the meta splittings at any temperature indicates a different arrangement in **4**. In other words the transition state, instead of the ground state, occurs in **4** when the two planes are nearly orthogonal. Owing to the steric repulsion of the pair of the ortho *tert*-butyl groups of one phenyl ring upon those of the other, the molecular model seems indeed to support the conclusion that a nearly coplanar conformation might be equally or even less crowded than an orthogonal one.

**Chart VII**

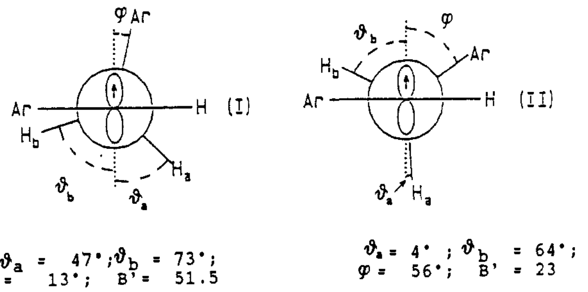

On the other hand, the rotational process about the $\mathrm{\dot{C}H{-}CH_2}$ bond can be described as due to the exchange between two identical conformers, each of which has two different $H_\beta$ splittings. The structure of such conformers can be obtained by means of the McConnell equation[32,33]

$$a^i_{H\beta} = A + \rho B \cos^2 \theta_i \quad i = \mathrm{a, b}$$

where $\theta_i$ represents the dihedral angle formed by the $CH^a_\beta$ (or the $CH^b_\beta$) bond with the $p_z$ orbital of the $\alpha$-carbon, $\rho$ is the spin density on $C_\alpha$, and $A$ and $B$ are empirical constants for a given class of radicals. The term $A$ is known to be small[19,34,35] (sometimes is even neglected[23,36]) with a generally accepted value[26,27,37] of 3 ± 2 G. The term $B' = \rho B$ can be estimated on the basis of an appropriate model in which a methyl group bonded to $C_\alpha$ can be assumed to freely rotate. In this situation it has been shown[19,35] that the methyl splitting $a_{Me}$ is equal to $A + {}^1/_2B'$. For unconjugated radicals (where $\rho = 1$, thus $B' = B$) the model of choice is the ethyl radical $\mathrm{\dot{C}H_2CH_3}$. From the corresponding methyl splitting ($a_{Me}$ = 27 G)[38] the term $B = B'$ is thus 48 G,[26] if $A$ = 3 G. On the other hand, for radicals where conjugation occurs,[35,36] as benzylic radicals, the appropriate model is phenylethyl radical ($\mathrm{Ph{-}\dot{C}H{-}CH_3}$) with an $a_{Me}$ value[37] of 17.9 G. Accordingly $B'$ is ~30 G (if $A$ = 3 G) for this class of radicals. This implies that the spin density $\rho$ is smaller than unity, in agreement with the fact that the $a_{H_\alpha}$ splitting in $\mathrm{Ph\dot{C}HCH_3}$ (16.3 G)[39] is smaller than that of $\mathrm{\dot{C}H_2CH_3}$ (22.4 G).[38]

In the case of radical **4**, however, two different $a_{H_\beta}$ splittings were measured, so that a system with two independent McConnell equations is available.[19,35] Assuming $A$ = 3 G, the values of $B'$ and $\theta_i$ ($\theta_a$ is dependent on $\theta_b$ because each of the three bond angles of the sp$^3$ $\beta$-carbon expressed in the Newman projection is equal to 120°) can be simultaneously calculated (Chart VII). The two values measured at −100 °C (25.9 and 7.4 G) yield two possible solutions[40] corresponding to conformers I and II of Chart VII that

---

[18] Schluter, K.; Berndt, A. *Tetrahedron Lett.* **1979**, 929.

[19] Lunazzi, L.; Placucci, G.; Grossi, L.; Guerra, M. *J. Chem. Soc., Perkin Trans. 2* **1982**, 43.

[20] Placucci, G.; Grossi, L. *Gazz. Chim. Ital.* **1982**, *112*, 375.

[21] Brumby, S. *J. Phys. Chem.* **1983**, *87*, 917.

[22] Ingold, K. U.; Nonhebel, D. C., Wildman, T. A. *J. Phys. Chem.* **1984**, *88*, 1675.

[23] Krusic, P. J.; Kochi, J. K. *J. Am. Chem. Soc.* **1971**, *93*, 846.

[24] Kochi, J. K.; Krusic, P. J. *Spec. Publ.—Chem. Soc.* **1971**, *24*, 147.

[25] Lunazzi, L.; Ingold, K. U. *J. Am. Chem. Soc.* **1972**, *94*, 8065.

[26] Griller, D.; Ingold, K. U. *J. Am. Chem. Soc.* **1974**, *96*, 6715.

[27] Griller, D.; Barclay, L. R. C.; Ingold, K. U. *J. Am. Chem. Soc.* **1975**, *97*, 6151.

[28] Casarini, D.; Lunazzi, L.; Placucci, G.; Ishida, T.; Ishii, A.; Okazaki, R. *J. Org. Chem.* **1988**, *53*, 1582.

[29] Berndt, A. In *Landolt-Bornstein New Series*; Springer Verlag: Berlin, Heidelberg, 1977; Vol. II/9b, p 562.

[30] Photolysis of ArCH═S (Ar = 2,4,6-tri-*tert*-butylphenyl) in EtOH/EtOK is known[28] to produce the corresponding radical anion $\mathrm{Ar\dot{C}HS^-}$. The latter, by reaction with the OH proton of EtOH, is transformed into $\mathrm{ArCH_2\dot{S}}$ which, by loss of sulfur, eventually gives $\mathrm{Ar\dot{C}H_2}$ (or $\mathrm{Ar\dot{C}HD}$ if EtOD is employed). As will be shown in a forthcoming paper, it is possible for $\mathrm{Ar\dot{C}H_2}$ to react with $\mathrm{Ar\dot{C}HS^-}$ to give $\mathrm{ArCH_2{-}CH(S^-)Ar}$, which eventually decomposes to yield $\mathrm{ArCH_2{-}\dot{C}HAr}$ (**4**), in a steady-state concentration large enough to be detected by ESR spectroscopy. Indeed, photolysis of ArCH═S in EtOD/EtOK yields the two equally intense ESR spectra expected for $\mathrm{ArCHD{-}\dot{C}HAr}$ (**4a**), whereas photolysis of ArCD═S in EtOH/EtOK yields the two equally intense spectra of $\mathrm{ArCHD{-}\dot{C}DAr}$ (**4b**). The existence of such pairs of ESR spectra for **4a** and **4b** depends upon the equal probability that the deuteron replaces the hydrogen responsible either for the larger or for the smaller of the two different $H_\beta$ splittings of **4**. Finally, photolysis of ArCD═S in EtOD/EtOK yields the single spectrum corresponding to $\mathrm{ArCD_2{-}\dot{C}DAr}$ (**4c**).

[31] Reference 29, pp 552, 556.

[32] Heller, C.; McConnell, H. M. *J. Chem. Phys.* **1960**, *32*, 1535.

[33] Although, in principle, more sophisticated approaches[19,34] should be used, this equation is still satisfactory for hydrocarbon radicals.

[34] Guerra, M. *Chem. Phys. Lett.* **1987**, *139*, 563.

[35] Lunazzi, L.; Placucci, G.; Grossi, L. *J. Chem. Soc., Perkin Trans. 2* **1980**, 1063.

[36] Leardini, R.; Tundo, A.; Zanardi, G.; Pedulli, G. F. *J. Chem. Soc., Perkin Trans. 2* **1983**, 285.

[37] Fischer, H. In *Free Radicals*; Kochi, J. K., Ed.; Wiley: New York, 1973; Vol. 2, Chapter 19.

[38] Fessenden, R. W. *J. Phys. Chem.* **1967**, *71*, 74; *J. Magn. Reson.* **1969**, *1*, 1277. Chen, K. S.; Kochi, J. K. *J. Am. Chem. Soc.* **1974**, *96*, 794.

[39] Greatorex, D.; Kemp, T. J. *Trans. Faraday Soc.* **1971**, *67*, 1576. Dobbs, A. J.; Gilber, B. C.; Norman, R. O. C. *J. Chem. Soc., Perkin Trans. 2* **1972**, 786.

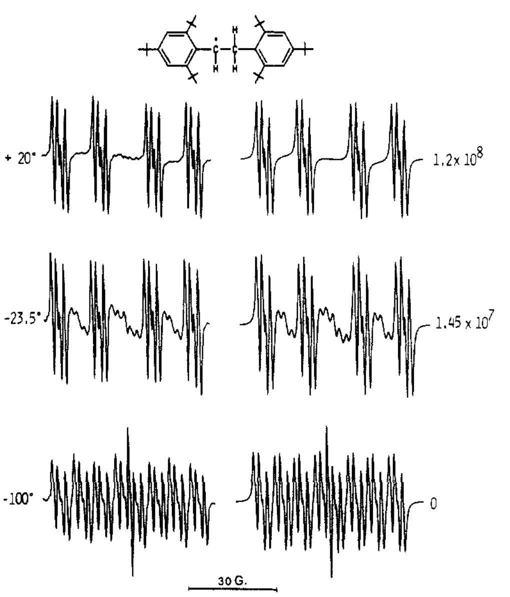

**Figure 3.** Experimental (left) and computed (right) ESR spectra of radical **4** in cyclopropane at various temperatures. The rate constants ($k$, s$^{-1}$) used for the simulations are also reported.

are related by a 43° clockwise rotation.

Conformer I looks more hindered than II and thus seems a less likely solution. A more solid argument can, however, be put forward to support the preference for conformer II. The term $B'$ (obtained by solving the pair of McConnell equations) turns out to be 51.5 G in the case of I, i.e., a value close to that estimated for the ethyl radical. Such a solution would thus imply that in **4** there is no delocalization of the unpaired electron on the Ar group. On the contrary the term $B' = 23$ G obtained for conformer II is closer to that of the conjugated benzylic radicals: this solution requires that radical **4** be considered a system where the unpaired electron is delocalized on the Ar group. The $a_{H_\alpha}$ splitting of **4** (14.25 G) is indeed much closer to those measured in benzylic radicals (16.3 G in $\text{Ph}\dot{\text{C}}\text{HCH}_3$[39] or 15.3 G in $\text{Ar}\dot{\text{C}}\text{H}_2$[27]) than in unconjugated alkyl radicals (22.4 G in $\dot{\text{C}}\text{H}_2\text{CH}_3$[38] or 22.1 G in $\text{CH}_3\dot{\text{C}}\text{HCH}_2\text{CH}_3$[41]). Furthermore, conformer II also agrees with the existence of two different meta splittings in **4**, a situation requiring a nearly coplanar arrangement of the Ar group[27] (see Chart VI), which obviously favors the delocalization of the unpaired electron. Little doubt seems left that radical **4** adopts conformation II.

A 68° clockwise rotation will produce an identical conformer where, however, $H_b$ has taken the place of $H_a$. Such a motion exchanges the two $H_\beta$ splittings, thus accounting for the line-width alternation observed in the ESR spectrum of **4** when the temperature is raised.

In Figure 3 the experimental and computed spectra of **4** are reported at three temperatures. By computer simulation various rate constants were actually obtained, thus allowing us to measure, in addition to $\Delta G^\ddagger$ (6.3 ± 0.15 kcal mol$^{-1}$), also the values of $\Delta H^\ddagger$ (6.3 ± 0.3 kcal mol$^{-1}$) and $\Delta S^\ddagger$ (−0.2 ± 1.0 eu). As expected for a torsional process of this type, the activation entropy is negligible.

By making use of the 3,5-dideuteriated ArCHS derivative[28] the radical **4d** was also observed: The corresponding ESR spectrum differs from that of **4** since the two meta splittings (1.75 and 2.6 G) disappear under the line width. Although the spectral shape of **4d** becomes, consequently, completely different from that of **4** in the region where exchange occurs, all the activation parameters were found equal. This places additional confidence on the stereodynamical data obtained for the torsional process occurring in this hindered radical.

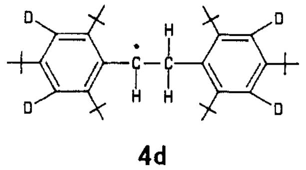

**4d**

## Experimental Section

**Material.** The preparation of **1,2-bis(2,4,6-tri-*tert*-butylphenyl)ethane (1)** has been reported.[11a]

**Bis(2,4,6-tri-*tert*-butylbenzyl) Sulfide (2).** To a tetrahydrofuran (THF) solution of sodium (2,4,6-tri-*tert*-butylphenyl)methanethiolate, prepared by adding a THF solution of **3** (26.8 mg, 0.046 mmol) to sodium (6.9 mg, 0.30 mmol) in liquid ammonia (−78 °C) and subsequent evaporation of ammonia and addition of THF, was added a THF solution of 2,4,6-tri-*tert*-butylbenzyl bromide (41.6 mg, 0.122 mmol). The reaction mixture was refluxed for 1.5 h and then quenched with aqueous $\text{NH}_4\text{Cl}$. The THF was evaporated, and the residue was extracted with dichloromethane. The residue obtained by evaporation of the dichloromethane solution was subjected to purification by preparative high-pressure liquid chromatography [column, Japan Analytical Industry, JAIGEL 1H) (styrene–divinylbenzene copolymer, pore size 25 Å)] to give **2** (19 mg, 0.034 mmol, 75%): mp 238.5–242 °C (hexane); $^1$H NMR ($\text{CDCl}_3$) $\delta$ 1.12 (s, 18 H), 1.37 (s, 36 H), 4.26 (br s, 4 H), 7.28 (br s 4 H); $^{13}$C NMR ($\text{CDCl}_3$) $\delta$ 31.4, 33.6, 34.8, 35.6, 37.7, 123.0, 131.8, 147.4, 149.3; MS $m/z$ (rel intensity) 550 (M$^+$, 6), 516 (11), 259 (63), 57 (100); HRMS calcd for $\text{C}_{38}\text{H}_{62}\text{S}$ (M$^+$) 550.4572, found 550.4590.

**Bis(2,4,6-tri-*tert*-butylbenzyl) Disulfide (3).** To a suspension of lithium aluminum hydride (86.1 mg, 2.1 mmol) in THF was added 2,4,6-tri-*tert*-butylthiobenzaldehyde[42] (1.17 g, 4.0 mmol) in THF (12 mL), and the mixture was stirred for 2 h at room temperature. An aqueous $\text{NH}_4\text{Cl}$ solution was added to the reaction solution, and the THF was evaporated. The residue was extracted with dichloromethane, and the organic layer was dried with anhydrous $\text{MgSO}_4$. After evaporation of the solution (2,4,6-tri-*tert*-butylphenyl)methanethiol was obtained quantitatively as white crystals: mp 100–102 °C (methanol); $^1$H NMR ($\text{CCl}_4$) $\delta$ 1.27 (s, 9 H), 1.43 (t, $J$ = 6 Hz, 1 H), 1.50 (s, 18 H), 4.22 (d, $J$ = 6 Hz, 2 H), 7.11 (s, 2 H); MS $m/z$ (rel intensity) 292 (M$^+$, 20.1), 243 (100). Anal. Calcd for $\text{C}_{19}\text{H}_{32}\text{S}$: C, 78.01; H, 11.03; S, 10.96. Found: C, 78.21; H, 11.27; S, 10.92.

To a benzene solution (2 mL) of the thiol (148 mg, 0.50 mmol) and triethylamine (0.084 mL, 0.61 mmol) was added a benzene solution of iodine (140 mg, 0.55 mmol) at room temperature. After being washed with aqueous sodium thiosulfate, the reaction mixture was evaporated and the residual crude product was recrystallized from ethanol to give **3** (90 mg, 62%): mp 190.2–192.6 °C; $^1$H NMR ($\text{CDCl}_3$) $\delta$ 1.29 (s, 18 H), 1.57 (s, 36 H), 4.77 (s, 4 H), 7.34 (s, 4 H); $^{13}$C NMR ($\text{CDCl}_3$) $\delta$ 31.4, 33.6, 34.9, 37.7, 42.2, 123.1, 129.9, 148.4, 149.5; MS $m/z$ (rel intensity) 582 (M$^+$, 0.4), 567 (0.1), 259 (100), 243 (40), 57 (38); HRMS calcd for $\text{C}_{38}\text{H}_{62}\text{S}_2$ (M$^+$) 582.4290, found 582.4268.

**Spectral Measurements.** The variable-temperature NMR spectra of **1–3** were obtained at 200 and 50.3 MHz for $^1$H and $^{13}$C, respectively (Varian, Gemini). The temperature was calibrated by inserting a thermistor into the probe or, alternatively, by using the temperature-dependent chemical shifts of methanol ($^1$H) or 2-chlorobutane ($^{13}$C).[43] When a gaseous solvent had to be used ($\text{CHF}_2\text{Cl}$, $\text{CCl}_2\text{F}_2$, or $\text{CHFCl}_2$), a 5-mm tube was connected to a vacuum line and the gas was condensed by means of liquid nitrogen. The tube was then sealed in vacuo and introduced in the precooled probe of the spectrometer. The exchanging signals of the methylene hydrogens were simulated assuming the AB approximation: at the coalescence, it was checked that the same rate constant is obtained with the AA′ BB′ formalism.

The ESR spectra of radical **4** were obtained by photolyzing a cyclopropane alkaline (EtOK/EtOH) solution of 2,4,6-tri-*tert*-butylthiobenzaldehyde[28] (using quartz tubes sealed in vacuo) within the cavity of a Varian E-3 spectrometer. At first the spectrum of the radical anion of $\text{Ar–}\dot{\text{C}}\text{H–S}^-$ is observed.[28] Under continuous photolysis the intensity of this spectrum decreases and the spectrum of **4** becomes visible. When the photolysis is interrupted the spectrum of the radical anion slowly disappears and that of the radical **4** becomes eventually the only de-

---

(40) There are two other possible solutions (conformers I′ and II′) having the same $\theta_i$ angles as I and II. They derive from I and II by a $2\phi$ anticlockwise rotation. Thus, I′ is obtained from I by a 26° rotation and II′ from II by a 112° rotation. Both I′ and II′ have, however, the two Ar groups extremely close to each other (the dihedral angle Ar–C–C–Ar would be 77° in I′, rather than 103° as in I, and 34° in II′, rather than 146° as in II) and were thus considered not acceptable on steric grounds.

(41) Chen, K. S.; Battioni, J. P.; Kochi, J. K. *J. Am. Chem. Soc.* **1973**, *95*, 4439.

(42) Okazaki, R.; Ishii, A.; Fukuda, N.; Oyama, H.; Inamoto, N. *J. Chem. Soc., Chem. Commun.* **1982**, 1187.

(43) Calibration kindly made available by Dr. J. E. Anderson, University College, London, U.K.

tectable spectrum (Figure 3). Radical **4** is persistent under these conditions for a few days. The temperature was monitored by inserting a thermocouple in the place of the sample before or after each spectral determination.

**Acknowledgment.** Thanks are due to the Ministry of Scientific Research (MURST), Rome and to the Italian CNR (Strategic Project "Electron Transfer") for financial support.

**Registry No. 1**, 83103-44-0; **2**, 125496-12-0; **3**, 19715-27-6; **4**, 125496-13-1; **4d**, 125496-14-2; sodium (2,4,6-tri-*tert*-butylphenyl)-methanethiolate, 125496-15-3; 2,4,6-tri-*tert*-butylbenzyl bromide, 125496-16-4; 2,4,6-tri-*tert*-butylthiobenzaldehyde, 84543-57-7; (2,4,6-tri-*tert*-butylphenyl)methanethiol, 125496-17-5.

---

# X-ray Absorption Spectral Study of Ferric High-Spin Hemoproteins: XANES Evidences for Coordination Structure of the Heme Iron

**Yoshitsugu Shiro,[*,†] Fumitoshi Sato,[‡] Tomohiko Suzuki,[§] Tetsutaro Iizuka,[*,†]
Tadashi Matsushita,[⊥] and Hiroyuki Oyanagi[‖]**

*Contribution from the Institute of Physical and Chemical Research, Wako, Saitama 351-01, Japan, Department of Physics, Faculty of Science and Technology, Keio University, Kohokuku, Yokohama 223, Japan, Department of Biology, Faculty of Science, Kochi University, Kochi 780, Japan, National Laboratory for High Energy Physics, Tsukuba, Ibaragi 305, Japan, and Electrotechnical Laboratory, Tsukuba, Ibaragi 305, Japan.* *Received August 7, 1989*

**Abstract:** The Fe XANES (X-ray absorption near-edge structure) spectra were measured at 80 K for hemoproteins in a ferric high-spin state. As ferric hemoproteins, we chose sperm whale myoglobin (Mb), its derivative modified at the distal histidine (His) by cyanogen bromide (BrCN–Mb), *Aplysia* Mb, and horseradish peroxidase (HRP), which have different structures at the heme distal side. In comparison of the spectra among the three Mbs, we found that the spectral features, in particular the intensities of the preedge P peak and the fine structure $C_1$ at the K-edge absorption, serve as a sensitive probe for the iron six-coordination structure; intense P and weak $C_1$ correspond to five-coordinated iron, while weak P and intense $C_1$ to six-coordination. Comparing the XANES spectrum of HRP with those of three Mbs, we suggested that the water molecule is absent at the sixth site of HRP, with pentacoordination of the heme iron.

X-ray diffraction has long been applied to a variety of protein single crystals to determine their three-dimensional structures.[1-3] Most attempts to explain protein or enzyme function have been based on the static structure obtained by these studies.[4] However, it is now recognized that conformation of the protein in a solution state is dynamically fluctuating and, as a consequence, it can readily associate or dissociate substrates and/or ligands.

X-ray absorption spectroscopy, with synchrotron radiation, is a powerful emerging technique for high-resolution studies of metal binding sites in proteins because a specific metal serves as a probe in a large molecular system.[5] The spectroscopy gives information on the local structure around the metal binding site, being sensitive to short-range order in atomic arrangements rather than to long-range order. Recently, this technique has been used for the study of hemoproteins in the solution state, especially for determining the local structure at the active site of such compounds as iron porphyrin.[6] In particular, the spectrum in the region of X-ray absorptin near-edge structure (XANES) contains information on the coordination geometry of the heme iron such as the Fe–ligand bond angle and on the distortion of symmetry due to small atomic displacement around the iron.[7,8]

We report here the XANES spectra of four hemoproteins in a ferric high-spin state: sperm whale myoglobin (Mb), its derivative chemically modified at its distal histidyl imidazole by cyanogen bromide (BrCN–Mb),[9] *Aplysia* Mb, and horseradish peroxidase (HRP). These hemoproteins have different types of structure at the heme distal side, although the heme iron of these four proteins has protoporphyrin IX as a planar ligand and a histidyl imidazole as the fifth ligand. (Detailed structures will

---

[*] To whom correspondence should be addressed.

[†] Institute of Physical and Chemical Research.

[‡] Keio University.

[§] Kochi University.

[⊥] National Laboratory for High Energy Physics.

[‖] Electrotechnical Laboratory.

(1) (a) Poulos, T. L.; Freer, S. T.; Alden, R. A.; Edwards, S. L.; Skoglund, U.; Takio, K.; Eriksson, B.; Xuong, N.-h.; Yonetani, T.; Kraut, J. *J. Biol. Chem.* **1980**, *255*, 575–580. (b) Finzel, B. C.; Poulos, T. L.; Kraut, J. *Ibid.* **1984**, *259*, 13027–13036. (c) Edwards, S. L.; Poulos, T. L.; Kraut, J. *Ibid.* **1984**, *259*, 12984–12988. (d) Edwards, S. L.; Xuong, N.-h.; Hamlin, R. C.; Kraut, J. *Biochemistry* **1987**, *26*, 1503–1511. (e) Poulos, T. L.; Finzel, B. C.; Gunsalus, I. C.; Wagner, G. C.; Kraut, J. *J. Biol. Chem.* **1985**, *260*, 16122–16130. (f) Poulos, T. L.; Finzel, B. C.; Howard, A. J. *J. Mol. Biol.* **1987**, *195*, 687–700. (g) Poulos, T. L.; Howard, A. J. *Biochemistry* **1987**, *26*, 8165–8174. (h) Fermi, G.; Perutz, M. F.; Shaanan, B. *J. Mol. Biol.* **1984**, *175*, 159–174. (i) Shaanan, B. *Ibid.* **1983**, *171*, 31–59.

(2) (a) Takano, T. *J. Mol. Biol.* **1977**, *110*, 537–568; (b) 569–584.

(3) (a) Bolognesi, M.; Coda, A.; Gatti, G.; Ascenzi, P.; Brunori, M. *Ibid.* **1985**, *183*, 113–115. (b) Bolognesi, M.; Onesti, S.; Gatti, G.; Coda, A.; Ascenzi, P.; Brunori, M. *Ibid.* **1989**, *205*, 529–544.

(4) Perutz, M. F. *Nature* (*London*) **1970**, *228*, 726–739.

(5) Bianconi, A.; Giovannelli, A.; Castellani, L.; Alema, S.; Fasella, P.; Oesch, B.; Mobilio, S. *J. Mol. Biol.* **1983**, *165*, 125–138.

(6) (a) Chance, B.; Fishetti, R.; Powers, L. *Biochemistry* **1983**, *22*, 3820–3829. (b) Powers, L.; Sessler, J. L.; Woolery, G. L.; Chance, B. *Ibid.* **1984**, *23*, 5519–5523. (c) Chance, M. R.; Parkhurst, L. J.; Powers, L. S.; Chance, B. *J. Biol. Chem.* **1986**, *261*, 5689–5692. (d) Perutz, M. F.; Hasnain, S. S.; Duke, P. J.; Sessler, J. L.; Hahn, J. E. *Nature* (*London*) **1982**, *295*, 535–538.

(7) (a) Pin, S.; Alpert, B.; Michalowicz, A. *FEBS Lett.* **1982**, *147*, 106–110. (b) Bianconi, A.; Congiu-Castellano, A.; Dell'Ariccia, M.; Giovannelli, A.; Durham, P. J.; Burattini, E.; Barteri, M. *FEBS Lett.* **1984**, *178*, 165–170. (c) Bianconi, A.; Congiu-Castellano, A.; Dell'Ariccia, M.; Giovannelli, A.; Burattini, E.; Durham, P. J. *Biochem. Biophys. Res. Commun.* **1985**, *131*, 98–102. (d) Bianconi, A.; Congiu-Castellano, A.; Dell'Ariccia, M.; Giovannelli, A.; Burattini, E.; Castagnola, M.; Durham, P. J. *Biochim. Biophys. Acta* **1985**, *831*, 12–124. (e) Pin, S.; Valat, P.; Cortes, R.; Michalowicz, A.; Alpert, B. *Biophys. J.* **1985**, *48*, 997–1001. (f) Bianconi, A.; Congiu-Castellano, A.; Durham, P. J.; Hasnain, S. S.; Phillips, S. *Nature* (*London*) **1985**, *318*, 685–687. (g) Congiu-Castellano, A.; Bianconi, A.; Dell'Ariccia, M.; Della Longa, S.; Giovannelli, A.; Burattini, E.; Castagnola, M. *Biochem. Biophys. Res. Commun.* **1987**, *147*, 31–38.

0002-7863/90/1512-2921$02.50/0